FEBS Letters 494 (2001) 150–156 FEBS 24748

A small peptide derived from Flt-1 (VEGFR-1) functions as an angiogenic inhibitor

Darren C.W. Tan[a], R. Manjunatha Kini[a], Seetharama D.S. Jois[b], Derrick K.F. Lim[a], Lixia Xin[a], Ruowen Ge[a,*]

[a] *Department of Biological Sciences, National University of Singapore, Singapore 119260, Singapore*
[b] *Department of Pharmacy, National University of Singapore, Singapore 119260, Singapore*

Received 4 January 2001; revised 2 March 2001; accepted 9 March 2001

First published online 23 March 2001

Edited by Veli-Pekka Lehto

Abstract Vascular endothelial growth factor (VEGF) is an angiogenic stimulator which functions through two endothelial specific tyrosine kinase receptors, Flt-1 and Flk-1. In this work, we show that an 11-amino acid peptide derived from the second immunoglobulin-like domain of Flt-1 functions as an angiogenic inhibitor in chick chorioallantoic membrane and inhibited VEGF-induced vascular permeability in Miles' assay without binding to VEGF directly. Circular dichroism and nuclear magnetic resonance analyses indicate that this peptide forms a stable extended structure in solution, presumably β-sheet structure and is most likely existing as a dimer. Our results suggest that this small peptide functions as an angiogenic inhibitor by inhibiting VEGF function through a non-VEGF binding mechanism.

Key words: Vascular endothelial growth factor (vascular permeability factor); Flt-1(VEGFR-1); Angiogenesis; Miles' assay; Chick chorioallantoic membrane

1. Introduction

Vascular endothelial growth factor (VEGF) (vascular permeability factor (VPF)) is a prime regulator of vasculogenesis, angiogenesis and vascular permeability. It is a secreted growth factor which functions as either paracrine or autocrine signals. Native VEGF is a 40–45-kDa basic, heparin-binding, homodimeric glycoprotein. Alternative splicing of the mRNA results in six isoforms of VEGF proteins in human [1,2].

Two high affinity VEGF receptors have been identified: VEGFR-1 (Flt-1, fms-like-tyrosine kinase) and VEGFR-2 (Flk-1/KDR, fetal liver kinase/kinase insert domain-containing receptor) [1,2]. The expression of these receptors is largely limited to the surface of the blood vessel endothelial cells. in vitro, both quiescent and proliferating endothelial cells have been shown to display high affinity binding for VEGF. The expression of the VEGF receptors is no doubt one of the earliest events in endothelial cell differentiation [3,4]. Both Flt-1 and Flk-1/KDR belong to the receptor tyrosine kinase (RTK) superfamily and contain seven extracellular immunoglobulin (Ig)-like domains, a single transmembrane region and two cytoplasmic tyrosine kinase domains separated by a kinase insert domain. VEGF effects its bioactivity by inducing receptor dimerization and tyrosine autophosphorylation of the kinase domains. This in turn induces a cascade of signal transductions that are not well understood.

Tumor growth and metastasis is angiogenesis dependent. VEGF is up-regulated in many tumors and plays critical roles in stimulating tumor angiogenesis [5]. In addition, its vascular permeability effect causes 'leakiness' in the incomplete basement membrane of the newly formed tumor capillaries thus facilitating metastasis [6]. Dominant-negative Flk-1 potently inhibits tumor growth [7–9]. A small peptide derived from the third Ig loop of Flk-1 inhibited $VEGF_{165}$-stimulated signal transduction and endothelial cell proliferation and migration [10]. Similarly, soluble Flt-1 inhibits retinal neovascularization and tumor angiogenesis [11,12]. Domain deletion studies of Flt-1 have demonstrated that the ligand-binding function resides in the first three Ig-like domains [1,13,14] and the 2nd Ig-like domain ($Flt\text{-}1_{D2}$) seems to play the most important role amongst the three domains by determining the ligand specificity of this receptor [15]. A complete and properly folded recombinant $Flt\text{-}1_{D2}$ is reported to be the minimum domain required to bind VEGF and it binds VEGF at 60-fold lower affinity compared to wild-type receptor [16].

In this work, we show an 11-amino acid small peptide derived from $Flt\text{-}1_{D2}$ can function as an angiogenic inhibitor in vivo. Interestingly, this peptide exhibits its effects without binding to VEGF or inhibiting VEGF's binding to its receptors.

2. Materials and methods

2.1. Peptide synthesis and purification

All the peptides were synthesized by a 433A peptide synthesizer (Applied Biosystems Inc., USA). Database searches determined the uniqueness of the peptides. The scrambled peptide is unique on its own with no protein matches. The peptides were purified using high pressure liquid chromatography (HPLC) on reversed-phase column C18 using an acetonitrile gradient. The sequences of all peptides were confirmed by their mass determined using electrospray mass spectrometry.

*Corresponding author. Fax: (65)-779-2486.
E-mail: dbsgerw@nus.edu.sg

Abbreviations: VEGF, vascular endothelial growth factor; VPF, vascular permeability factor; HUVEC, human umbilical cord vascular endothelial cells; CAM, chick chorioallantoic membrane; CD, circular dichroism; NMR, nuclear magnetic resonance

0014-5793/01/$20.00
PII: S0014-5793(01)02314-6

2.2. Chick chorioallantoic membrane (CAM) in vivo angiogenesis assay

CAM assays were performed at both the 4th and 13th day of chick embryo development. Peptides dissolved in sterile water were air-dried onto sterile glass coverslides of approximately 1 mm^2. The coverslides were placed onto the well vascularized site of the CAM of the developing chick embryos. The possible anti-angiogenic response was evaluated 48 h later and recorded down with stereomicroscope photography (Leica MZ12, Switzerland). The positive anti-angiogenic effect was scored when microvessels under the coverslides were obviously reduced at 48 h after sample application on day 13 CAM or an obvious blockage of CAM vessel development was observed on day 4 CAM.

2.3. Miles' vascular permeability assay

Evans blue (0.5%) was injected intracardiacally into Hartley albino guinea pigs of about 300–350 g. Test or control samples in water (100 μl) were injected intradermally into shaved dorsal areas. 10 ng human recombinant $VEGF_{165}$ ($hrVEGF_{165}$; Sigma, USA) consistently induced intense vascular leakage within 5 min of application and was used in all experiments. Various peptides at 100×, 1000×, 10 000× or 100 000× molar excess was mixed with $hrVEGF_{165}$ for testing. All tests were done in duplicates in each experiment and repeated at least three times.

2.4. Binding assays of VEGF and peptides

VEGF binding to human umbilical cord vascular endothelial cells (HUVEC) was done essentially as previously described [17–20]. HUVECs (Clonetics, USA) were verified by their expression of endothelial cell specific markers such as von Willebrand factor (vWF) by immunostaining and Flt-1 by RT-PCR before used in binding experiments (data not shown). HUVECs (8×10^4) were seeded into 24-well plates coated with gelatin. The cells were then incubated in the complete culture medium (MCDB-131 plus 25 ng/ml aFGF, 50 μg/ml gentamicin, 17.6 U/ml heparin, 1% L-glutamine and 10% fetal bovine serum) overnight. Cells were washed thoroughly with PBS and I^{125}-VEGF (80 μCi/μg, NEN, USA) in 100 μl of binding buffer (MCDB-131+0.1% BSA) was added to the cells and incubated for 2 h at room temperature. Test peptide was pre-mixed with I^{125}-VEGF before adding to HUVECs. An anti-human VEGF neutralizing monoclonal antibody (R&D Systems, USA) was used as a positive control for inhibition. Following incubation, the cells were washed three times with PBS and lysed in the lysis buffer (0.5% SDS). Cell-bound I^{125}-VEGF was measured using an automatic γ-counter. All tests were performed in triplicates and repeated at least three times.

2.5. Structural analysis of the small peptides by circular dichroism (CD) and nuclear magnetic resonance (NMR)

CD studies of the peptides were carried out on a JASCO J-720 spectropolarimeter. Peptides samples were prepared in phosphate buffer at pH 7.0. Concentrations of the peptides were in the range of 1–1.2 mg/ml. Path length of the cell was 1 mm. Spectra were collected in the wavelength range of 200–280 nm. For dilution studies of the peptides, samples were diluted to 1/5 of the original concentration using phosphate buffer and spectra were recorded. Values of ellipticity were expressed as molar ellipticity deg cm^2/dmol. CD spectra of the peptides were also recorded at pH 4.5 to compare with the NMR results. Two-dimensional NMR spectra of the peptides were recorded using a 500-MHz Bruker-Avance spectrometer. Concentrations of the peptides were in the range of 1–1.4 mM. Peptides were dissolved in 90% H_2O/10% D_2O and pH was adjusted to 4.5. Water suppression was achieved by presaturation during relaxation delay. Processing of the NMR spectra was carried out using xwin NMR on silicon graphics computer.

3. Results

3.1. Small peptides derived from Flt-1_{D2} inhibited angiogenesis in CAM

Peptides were designed based on (1) Flt-1 VEGF-binding domain data by mutational analysis [15]; (2) the available VEGF-Flt-1_{D2} protein crystal structure [16] (Fig. 1B); (3) the finding that proline residues are commonly found in the flanking segments of protein–protein interaction sites [21]. According to the proline hypothesis and the amino acid sequence of Flt-1_{D2}, two sites were selected to be potential protein–protein interaction sites. Both peptides, Flt1-12 (12 amino acids) and Flt2-13 (13 amino acids), were synthesized and found to be highly soluble in H_2O (Fig. 1A). Database searches indicated that these peptide sequences are unique and found only in Flt-1_{D2}. While Flt2-13 showed anti-angiogenesis activity when tested on day 4 CAM, Flt1-12 is not active (Fig. 2A and data not shown). When Flt2-13 was then tested on day 13 CAM embryos, it resulted in angiogenesis inhibition as well as vessel regression after 48 h (Fig. 2B). A randomly scrambled Flt2-13 peptide (sFlt2-13) completely lost this angiogenesis inhibition/vessel regression induction activity (Figs. 1A and 2B). This indicated that the anti-angiogenic/vessel regression activity of peptide Flt2-13 is sequence dependent. Since proline brackets enhanced the potency of short bioactive peptides, we replaced the N-terminal proline into threonine [22]. As expected, peptide Flt2-13T had a reduced activity in CAM (Figs. 1A and 2B).

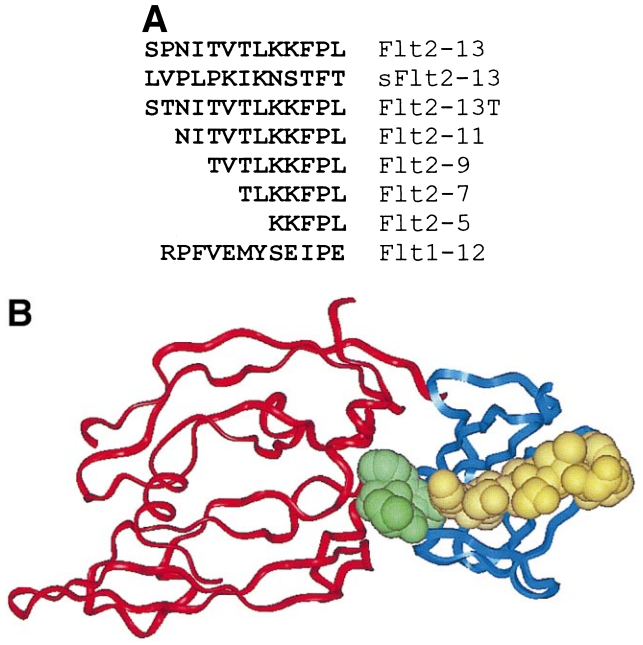

Fig. 1. A: Amino acid sequences of peptides. B: Three-dimensional structure of VEGF-Flt-1_{D2} complex. The original structure [16] is modified to show the relevant parts of the complex only. The VEGF molecule is in red and Flt-1_{D2} in blue. Peptide Flt2-11 is shown as CPK; green shows the C-terminal amino acids of Flt2-11 which are in contact with VEGF; yellow shows the rest of the amino acids in this peptide.

To determine the smallest peptide which still retains the angiogenesis inhibition/vessel regression activity, serial N-terminal truncations of peptide Flt2-13 were made and tested on day 13 CAM (Fig. 1A). Interestingly, peptide Flt2-11 showed more potent activity than Flt2-13 while peptide Flt2-9 showed comparable activity with Flt2-13 (Figs. 1A,B and 2B). Further truncations of the peptide (Flt2-7 and Flt2-5) destroyed this activity (data not shown). Application of the peptides sometimes caused non-specific opaque core formation, in a dose-dependent manner, which interfered in the data evaluation in CAM. Therefore, only samples which did not cause opaque core formation were recorded as having a positive vessel re-

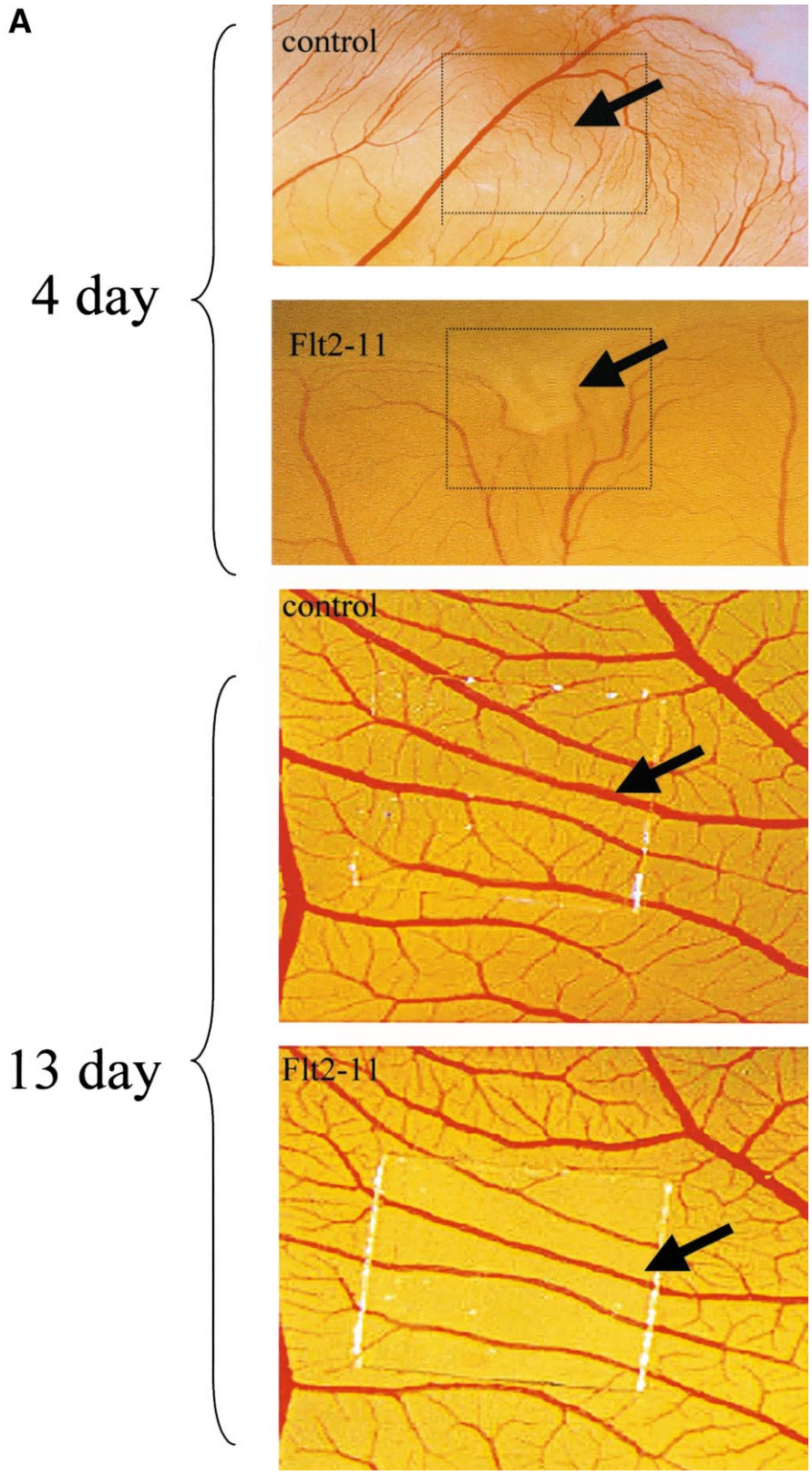

Fig. 2. A: Peptide Flt2-11 inhibited CAM angiogenesis on day 4 and induced vessel regression on day 13. Arrows indicate the reduced microvasculature 48 h after sample application to the CAM. B: Summary of the angiogenesis inhibition/vessel regression activity of various peptides on day 13 CAM. The *y*-axis indicates the percentage of samples that showed vessel regression induction activity. Error bars are standard errors. A minimum effective sample number of 20 is tested for each peptide at each dose from repeated experiments.

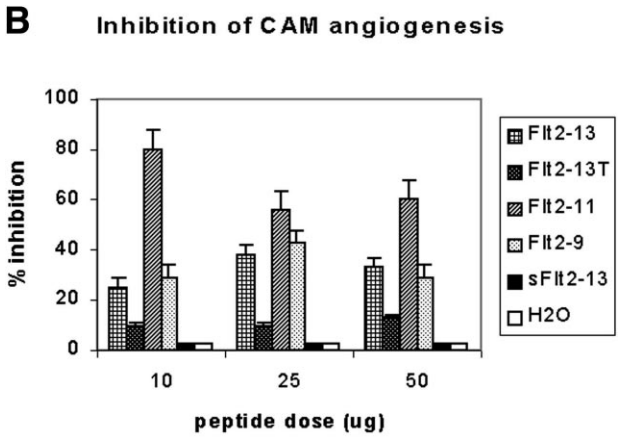

Fig. 2 (*continued*).

gression induction effect. This resulted in a less number of samples being counted in high peptide doses (25 and 50 μg), hence a lower percent of inhibition compared to 10 μg peptide (Fig. 2B and data not shown). However, the relative activities of the various peptides are generally consistent in the various doses tested. Thus three peptides derived from the same region of Flt-1_{D2}, at 13, 11 and 9 amino acids in length respectively, function as angiogenic inhibitors/vessel regression inducers in CAM. Amongst them, peptide Flt2-11 has the highest activity.

3.2. *Peptide Flt2-11 inhibits vascular permeability induced by VEGF*

The active anti-angiogenic peptides selected above were then tested on their ability to inhibit $hrVEGF_{165}$-induced vascular permeability using the Miles' vascular permeability assay [23,24]. 10 ng of $hrVEGF_{165}$ was injected intradermally into the dorsal or flanking skin of guinea pigs to induce a significant and consistent leakage of pre-injected Evan's blue dye within 5 min. The three peptides showed no induction of vascular leakage by themselves (data not shown).

Various doses of peptides were pre-mixed with $hrVEGF_{165}$ before injecting intradermally into guinea pigs. Only peptide Flt2-11 showed complete inhibition of $hrVEGF_{165}$-induced vascular hyperpermeability at 100 000-fold molar excess of VEGF. At this dose, no vascular leakage was observed even after 2 h of injection of hrVEGF (Fig. 3). Similar doses of four other peptides tested including Flt2-13, Flt2-9, Flt2-13T, Flt1-12 all failed to show any inhibitory effect under the same testing conditions (Fig. 3 and data not shown).

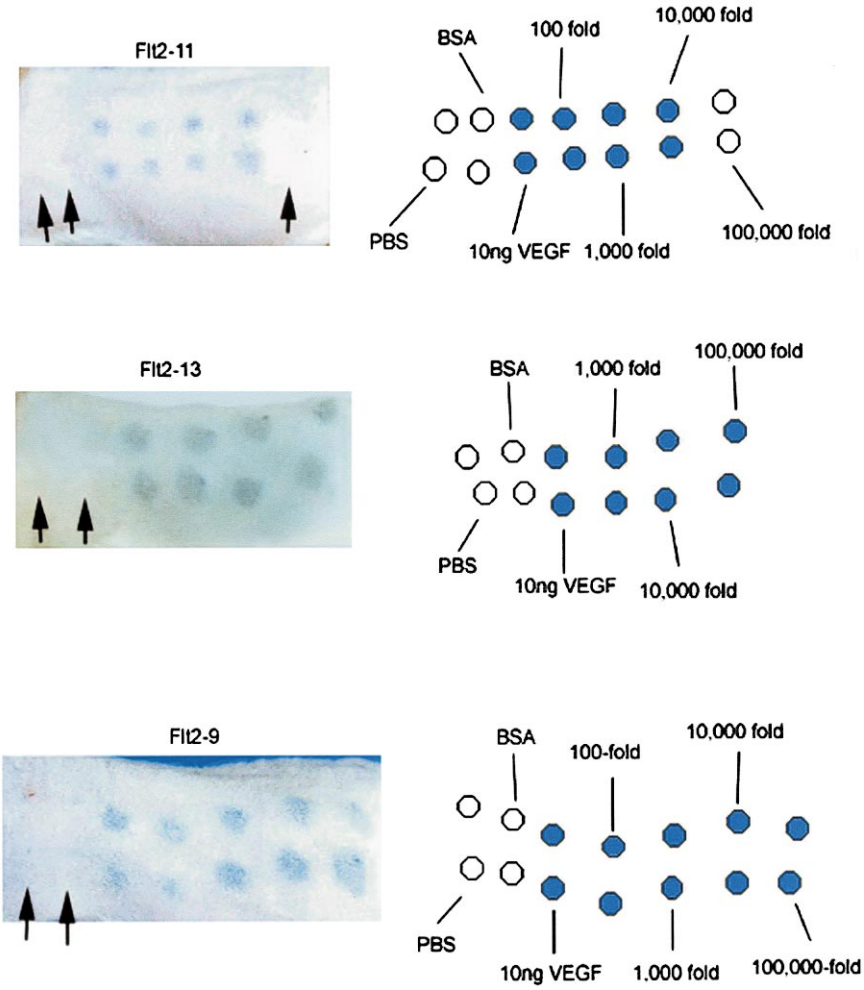

Fig. 3. Peptide Flt2-11 inhibited $VEGF_{165}$-induced vascular permeability in Miles' assay. Actual photos of the experiments are shown on the left and the schematic representations are shown on the right. Arrows indicate the positions in which injection of the samples produced no vascular leakage of the guinea pig skin. The fold numbers indicate the molar excess of peptide over recombinant human $VEGF_{165}$ in the samples.

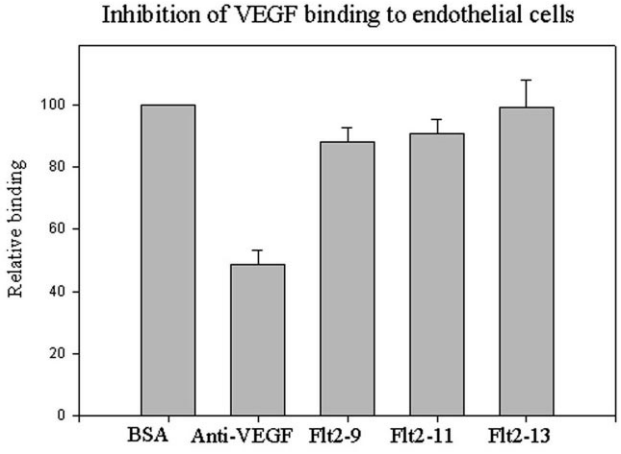

Fig. 4. $VEGF_{165}$ binding to HUVEC cells is not inhibited with excess peptides. $VEGF_{165}$ binding to HUVEC in the presence of BSA is taking as 100% binding. The bindings of $VEGF_{165}$ in the presence of 100 000-fold molar excess of various peptides as well as anti-VEGF antibody at 80 ng/ml were shown as percentage of the control binding. Error bars are standard errors.

These results indicate that peptide Flt2-11 was able to inhibit VEGF-induced vascular permeability in vivo. This is consistent with previous CAM assays, which showed that amongst all the peptides tested, Flt2-11 has the highest angiogenesis inhibitory activity.

3.3. Peptide Flt2-11 does not bind to VEGF nor does it inhibit VEGF's binding to its receptors on HUVEC cells

To test whether Flt2-11 inhibits VEGF function by interfering with VEGF binding to its receptors, we examined I^{125}-VEGF binding to HUVEC cells in the presence or absence of the peptides using identical experimental binding conditions used earlier where truncated Flt-1 (sFlt-1) has been shown to inhibit I^{125}-VEGF's binding to these cells [17–20]. The cells used were pre-tested for endothelial cell specific markers and expression of Flt-1 mRNA (data not shown). No peptides (including Flt2-11) showed significant inhibition of I^{125}-VEGF binding to HUVEC cells even at 100 000-fold molar excess (Fig. 4). In contrast, an anti-VEGF monoclonal antibody effectively inhibited I^{125}-VEGF binding under the same binding conditions.

The ability of the peptides to bind I^{125}-VEGF was also analyzed. Peptides were blotted onto a nitrocellulose membrane or coated onto the surface of a 96-well plate and then incubated with I^{125}-VEGF in binding buffers. No significant retention of I^{125}-VEGF was detected in either binding assays compared to BSA control even with very high amounts of peptides (data not shown). These results indicate that peptide Flt2-11 most likely neither binds to VEGF and nor does it interfere with VEGF's binding to its receptors on HUVEC cells.

3.4. Peptide Flt2-11 forms extended or β-sheet structure in solution

The three-dimensional structure shows that parts of peptide Flt2-11 reside at the third β-sheet in $Flt\text{-}1_{D2}$ [16]. The VEGF interaction site (residues 171–173) of $Flt\text{-}1_{D2}$ is localized at the C-terminal end of this peptide (Fig. 1B). To determine whether structural differences between the peptides could contribute to their anti-angiogenic activity, we examined their structures by CD and two-dimensional NMR. At 1.2 mg/ml, peptide Flt2-13 showed a negative band around 225–230 nm while peptides Flt2-11 and Flt2-9 showed two negative bands, one around 225–230 nm and the second band around 215–217 nm (Fig. 5A). Peptide Flt2-7 showed a small negative band around 230 nm and a large negative band around 210 nm. In the case of peptide Flt2-13, the negative band around 225 nm had an especially large intensity. The negative band around 225–230 nm usually indicates the possibility of peptide acquiring a β-turn structure [25]. As the peptide was truncated from the N-terminal end, the intensity of the 225-nm negative band decreased (Fig. 5A). In Flt2-11, in addition to the negative CD band at 228 nm, a new band at 217 nm appeared suggesting a β-sheet in addition to the β-turn structure. Peptide Flt2-9 showed similar spectrum to that of Flt2-11 with two negative bands, one around 228 nm and the other around 215 nm. In peptide Flt2-7, the negative band around 230 nm became very small in intensity and the intensity around the 210-nm band increased (Fig. 5A) indicating a more flexible/unordered structure. Upon dilution, the CD spectra of peptide Flt2-11 showed drastic changes in the intensity of the 225-nm negative band indicating loss of β-sheet conformation (Fig. 5B). The band around 205 nm suggested that upon dilution the peptide acquires a more flexible/unordered structure.

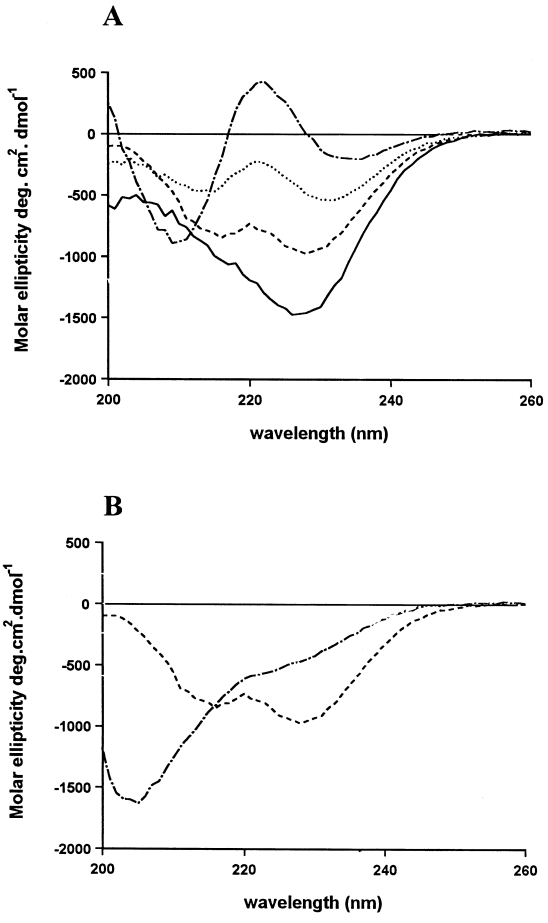

Fig. 5. CD spectra of the peptides in solution. A: CD spectra of various peptides at 1 mg/ml. Flt2-13 (–); Flt2-11 (-----); Flt2-9 (.....); Flt2-7 (–·). B: CD spectra of peptide Flt2-11 upon dilution of the peptide to 0.2 mg/ml indicating change in structure upon dilution. (-----) Peptide at 1 mg/ml; (–·) peptide at 0.2 mg/ml.

To further understand the secondary structure of the peptides, two-dimensional NMR studies were carried out. ROESY spectra of the peptides showed sequential connectivities indicating extended structure in the peptides. Peptide Flt2-13 showed NH–NH connectivities in the ROESY spectrum indicating the presence of β-turn in the peptide structure (data not shown). All the other three peptides (Flt2-11, Flt2-9 and Flt2-7) did not show any NH–NH connectivity suggesting that these peptides acquire an extended structure [26]. Combining the CD and NMR results, peptides Flt2-11, Flt2-9 and Flt2-7 most likely acquire extended (β-sheet) structure in solution at the higher concentration while peptide Flt2-13 may have a β-turn structure. It is interesting to note that it is unusual to observe such stable β-sheet structure of small peptides in solution. The detailed NMR analysis will be presented elsewhere.

4. Discussion

There have been reports of small peptides derived from large proteins which can function as inhibitors of the large proteins. For example, a 17-residue peptide derived from the third Ig-like domain of Flk-1 inhibited VEGF-stimulated autophosphorylation of Flk-1 (VEGFR-2) as well as proliferation and migration of cultured microvascular endothelial cells [10]. This Flk-1 peptide binds to VEGF and the covalently dimerized form of this peptide inhibited ^{125}I-VEGF binding to HUVEC cells. So this peptide functions as VEGF inhibitor by competitively binding to VEGF receptors on endothelial cells [10]. In another example, a peptide corresponding to $VEGF_{165}$ exon-7 inhibited VEGF function by inhibiting VEGF's binding to HUVEC cells [27].

In this work, we have identified an 11-amino acid peptide, Flt2-11, derived from the second Ig-like domain of human Flt-1 which can inhibit CAM angiogenesis as well as VEGF-induced vascular permeability. Although initial CAM angiogenesis assays showed that peptides Flt2-13, Flt2-11 and Flt2-9 all have angiogenesis inhibition/vessel regression activities, only Flt2-11 was able to inhibit VEGF-induced vascular permeability in Miles' assay. Incidentally, Flt2-11 also has the highest angiogenesis inhibition/vessel regression activity in CAM. The extreme high sensitivity and potency of VEGF induced vascular permeability in Miles' assay is probably the reason why high amounts of Flt2-11 peptide are needed to completely inhibit the dye leakage. Since this segment of Flt-1 was involved in the complex formation with VEGF [16], we expected the peptide to bind to VEGF and interfere with its interaction with Flt-1. Surprisingly, Flt-11 peptide does not bind to VEGF nor does it inhibit I^{125}-VEGF binding to HUVEC cells in our tested conditions. As peptide Flt2-11 contains no cysteine residues and therefore is not able to form any disulfide bond, our result is consistent with previous reports that a complete Flt-1_{D2} is the minimum domain required to bind VEGF [13,14,16]. Therefore, peptide Flt2-11 possibly interferes with VEGF-stimulated angiogenesis and vascular permeability through a non-VEGF binding mechanism.

The molecular mechanisms of VEGF-induced vascular permeability are not well understood. Particularly, the receptors involved in this VEGF signaling are essentially unknown. Recently, a VEGF mutant which lacks Flk-1 activation was shown to retain the ability to induce vascular permeability [28]. This finding uncouples VEGF-induced vascular leakage to mitogenesis. It seems possible then that VEGF induces vascular leakage through receptors other than Flk-1 on the endothelial cell surface such as Flt-1. However, as both placental growth factor (PlGF) and VEGF-B, members of the VEGF family which only bind Flt-1, lack any significant permeability inducing activity, whether Flt-1 is involved in VEGF-induced vascular leakage needs further investigation. In this regard, peptide Flt2-11 may be a useful tool to study the molecular mechanism of VEGF-induced vascular permeability.

CD and NMR analyses of the peptides indicate that Flt2-13 shows significant β-turn in its structure, whereas Flt2-11 and Flt2-9 form β-sheets in solution (Fig. 5). Further, peptide Flt2-11 most likely exists as a stable dimer in solution as shown by dilution experiments (Fig. 5B) and ROESY data (not shown). Interestingly, this increase in the extended β-sheet conformation in Flt2-11 showed concurrent increase in the anti-angiogenic effects. Further truncations of the peptides resulted in lower β-sheet content as well as decrease in activity. The decrease in β-sheet content can be explained by the decrease in the number of hydrogen bond interactions. Loss of critical amino acid or β-sheet structure during further truncation might explain the decrease or loss of anti-angiogenic activity in Flt2-9 and Flt2-7. It is important to note that these peptides still have the residues that are involved in 'actual' contact between VEGF and Flt-1_{D2} [16]. Our results indicate the extended structure in this segment somehow contributes to the inhibition of VEGF activity. On the other hand, Flt2-11 acts by a distinctly different mechanism other than one expected based on direct interaction, since it did not inhibit VEGF's binding to its receptors on HUVEC cells nor did it bind to VEGF itself. The contribution of the unusual, but stable β-sheets formed by dimeric interactions in solution is also not clear. The possibility that peptide Flt2-11 can interfere with VEGF receptor dimerization cannot be excluded. Our experiments also do not address the possible internalization and interference of intracellular signaling by this peptide. Further studies are needed to clarify these in order to understand the mechanism of this peptide inhibition of VEGF function. Irrespective, derivatives or mimics of this peptide with improved anti-angiogenic potency may help us to develop prototypes of anti-angiogenic drugs.

Acknowledgements: R.G. would like to thank the National University of Singapore for support of this research (RP950358 and RP981308).

References

[1] Ferrara, N. and Davis-Smyth, T. (1997) Endocr. Rev. 18, 4–25.
[2] Neufeld, G., Cohen, T., Gengrinovitch, S. and Poltorak, Z. (1999) FASEB J. 13, 9–22.
[3] Jakeman, L.B., Winer, J., Bennett, G.L., Altar, C.A. and Ferrara, N. (1992) J. Clin. Invest. 89, 244–253.
[4] Jakeman, L.B., Armanini, M., Phillips, H.S. and Ferrara, N. (1993) Endocrine 133, 848–859.
[5] Leenders, W.P.J. (1998) Int. J. Exp. Pathol. 79, 339–346.
[6] Dvorak, H.F., Brown, L.F., Nagy, J.A. Feng, D. and Dvorak, A.M. (1997) in: Vascular Endothelium, pp. 345–352, Born and Schwartz, Schattauer.
[7] Millauer, B., Shawver, L.K., Plate, K.H., Risau, W. and Ullrich, A. (1994) Nature 367, 576–579.
[8] Millauer, B., Longhi, M.P., Plate, K.H., Shawver, L.K., Risau, W., Ullrich, A. and Strawn, M.M. (1996) Cancer Res. 56, 1615–1620.

[9] Lin, P., Sanker, S., Shan, S.Q., Dewhirst, M.W., Polverini, P.J., Quinn, T.Q. and Peters, K.G. (1998) Cell Growth Differ. 9, 49–58.
[10] Piossek, C., Scheider-Mergener, J., Schirer, M., Vakalopoulou, E., Germeroth, L. and Thierauch, K.H. (1999) J. Biol. Chem. 274, 5612–5619.
[11] Aiello, L.P., Pierce, E.A., Foley, E.D., Takagi, H., Chen, H., Riddle, L., Ferrara, N., King, G.L. and Smith, L.E.H. (1995) Proc. Natl. Acad. Sci. USA 92, 10457–10461.
[12] Kong, H.-L., Hecht, D., Song, W., Kovesdi, I., Hackett, N.R., Yayon, A. and Crystal, R.G. (1998) Hum. Gene Ther. 9, 823–833.
[13] Barleon, B., Totzke, F., Herzog, C., Blanke, S., Kremmer, E., Siemeister, G., Marmé, D. and Martiny-Baron, G. (1997) J. Biol. Chem. 272, 10382–10388.
[14] Cunningham, S.A., Stephan, C.C., Arrate, M.P., Ayer, K.G. and Brock, T.A. (1997) Biochem. Biophys. Res. Commun. 231, 596–599.
[15] Davis-Smyth, T., Chen, H., Park, J., Presta, L.G. and Ferrara, N. (1996) EMBO J. 15, 4919–4927.
[16] Wiesmann, C., Fuh, G., Christinger, H.W., Eigenbrot, C., Wells, J.A. and de Vos, A.M. (1997) Cell 91, 695–704.
[17] Myoken, Y., Kayada, Y., Okamoto, T., Kan, M., Sato, G.H. and Sato, J.D. (1991) Proc. Natl. Acad. Sci. USA 88, 5819–5823.
[18] Kendall, R.L. and Thomas, K.A. (1993) Proc. Natl. Acad. Sci. USA 90, 10705–10709.
[19] Kendall, R.L. and Thomas, K.A. Jr. (1998) US patent # 5,712,380.
[20] Bikfalvi, A., Sauzeau, C., Moukadiri, H., Maclouf, J., Busso, N., Bryckaert, M., Plouet, J. and Tobelem, G. (1991) J. Cell. Physiol. 149, 50–59.
[21] Kini, R.M. and Evans, H.J. (1994) Curr. Top. Pept. Protein Res. 1, 297–311.
[22] Kini, R.M. and Evans, H.J. (1995) FEBS Lett. 375, 15–17.
[23] Miles, A.A. and Miles, E.M. (1952) J. Physiol. 118, 228–257.
[24] Keck, P.J., Hauser, S.D., Krivi, G., Sanzo, K., Warren, T., Feder, J. and Connolly, D.T. (1989) Science 246, 1309–1312.
[25] Fasman, G.D. (1996) Circular Dichroism and Conformational Analysis of Biomolecules, Plenum, New York.
[26] Wuthrich, K. (1986) NMR of Proteins and Nucleic Acids, John Wiley and Sons, New York.
[27] Soker, S., Gollamudi-Payne, S., Fidder, H., Charmahelli, H. and Klagsbrun, M. (1997) J. Biol. Chem. 272, 31582–31588.
[28] Stacker, S.A., Vitali, A., Caesar, C., Domagala, T., Groenen, L.C., Nice, E., Achen, M.G. and Wilks, A.F. (1999) J. Biol. Chem. 274, 34884–34892.